Chain configuration and flexibility gradient in phospholipid membranes

Comparison between spin-label electron spin resonance and deuteron nuclear magnetic resonance, and identification of new conformations

Michael Moser,* Derek Marsh,‡ Peter Meier,* Karl-Heinz Wassmer,* and Gerd Kothe*
*Institut für Physikalische Chemie der Universität Stuttgart, D-7000 Stuttgart 80, Federal Republic of Germany; ‡Abteilung Spektroskopie, Max-Planck-Institut für Biophysikalische Chemie, D-3400 Göttingen, Federal Republic of Germany

ABSTRACT The electron spin resonance spectra of 1-myristoyl-2-[*n*-(4,4-dimethyloxazolidine-*N*-oxyl)myristoyl]-*sn*-glycero-3-phosphocholine spin-label positional isomers (n = 6, 10, and 13) have been studied in oriented, fully hydrated bilayers of dimyristoylphosphatidylcholine, as a function of temperature and magnetic field orientation. The spectra have been simulated using a line-shape model which incorporates chain rotational isomerism, as well as restricted anisotropic motion of the lipid molecules as a whole, and which is valid in all motional regimes of conventional spin-label electron spin resonance (ESR) spectroscopy. At least one component of the lipid motion is found to lie in the slow-motion regime for all label positions, even in the fluid liquid crystalline phase, well above the phase transition. In the gel phase, the chain isomerism lies in the slow-motional regime, and the overall motions are at the rigid-limit. In the fluid phase, the chain isomerism is in the fast-motional regime, and the chain axis motions are in the slow regime. This indicates that the commonly used motional-narrowing theory is not appropriate for the interpretation of spin-label spectra in biological membranes. The simulation parameters yield a consistent description for the chain order and dynamics for all label positions. The correlation times and order parameters for the overall motion are the same at all positions down the chain, whereas the chain conformation and *trans-gauche* isomerism rate display a characteristic flexibility gradient, with increasing motion towards the terminal methyl end of the chain. Significantly, it is found that all six distinct tetrahedral orientations of the hyperfine tensor at the labeled segment are required for a consistent description of the chain isomerism. For the C-6 segment only the 0° (*trans*) and two 60° (*gauche*) orientations are significantly populated, for the C-10 position two further 60° orientations are populated, and for the C-13 position all orientations have non-vanishing populations. Detailed comparisons have been made with the results of ^{2}H nuclear magnetic resonance (NMR) measurements on dimyristoylphosphatidylcholine labeled at the same position in the *sn*-2 chain, and using an identical motional model. The parameters of overall reorientation, both order parameter and correlation times, have very similar values as determined by ESR and NMR. The major difference between the results from the two methods lies in the conformational populations at the labeled chain segment and the *trans-gauche* isomerization rate in the gel phase. The conformational order is much lower for the spin-labeled chain segments than for the corresponding deuterium-labeled segments, and the isomer interconversion rates in the gel phase (although displaying a mobility gradient in both cases) are found to be much slower in the former case. In addition the spin-label measurements provide information on the macroorder (chain tilt), which is only available from oriented samples. These results are consistent between the different spin-label positions and are in agreement with the findings from x-ray diffraction.

INTRODUCTION

A fluid lipid environment is essential for many critical membrane functions. Much information on the underlying molecular dynamics has been obtained from the study of lipid bilayer model membranes. The entropy changes taking place at the gel-to-fluid phase transition in lipid bilayers indicate that the molecular basis of the membrane fluidity is rotational isomerism in the lipid hydrocarbon chains (see, e.g., reference 1). Magnetic resonance and diffraction methods have indicated that the cumulative effect of rotational isomerism results in a characteristic flexibility gradient and a progressive chain shortening on proceeding down the length of the chain from the polar headgroup region to the terminal methyl groups (2–5). In addition to segmental motion, overall angular fluctuations may also take place, as well as rotations about the long axis of the lipid molecules. All of the above-mentioned angular rotational motions have been detected, or at least hinted at, by magnetic resonance spectroscopy (see, e.g., references 2, 3, 6, and 7). Chain rotational isomerism and limited angular fluctuations within an orienting potential are also common features of many of the statistical mechanical bilayer models used to interpret the thermodynamic and dimensional properties of lipid bilayers (reviewed in reference 1).

A detailed description of any aspect of the lipid molecular dynamics requires a comprehensive motional model to interpret the data from the magnetic resonance spectroscopic methods. To a certain extent this has already

0006-3495/89/01/111/13 $2.00

been undertaken in the analysis of ^2H nuclear magnetic resonance (NMR) (7, 8), and also of spin-label electron spin resonance (ESR) (6, 9, 10), for labeled lipid molecules. The purpose of the present paper is first to extend our previous measurements (6), particularly with spin-label ESR, to other positions of chain labeling and second, to provide a detailed comparison between the spin-label ESR and ^2H-NMR results on the chain order, conformation, and dynamics. The reason for doing the latter is not simply to assess the distorting effect of the spin-label group on the local chain conformation, but more importantly to check the results obtained on chain dynamics by two spectroscopic methods with considerably different ranges of motional sensitivity.

Previous, more limited, studies have indicated that, in spite of the presence of the spin-label group, the overall dynamics recorded by ESR are reasonably similar (within a factor of 2–3 in correlation times) to those obtained from ^2H-NMR (6). The advantage of using ESR to determine the lipid dynamics, therefore, lies not only in the better sensitivity relative to ^2H-NMR, but also in the fact that the characteristic timescale for nitroxide spin-label ESR (sensitivity to correlation times in the range ~0.1–100 ns) matches very closely the rates of molecular rotation observed in fluid lipid bilayers and membranes. Deuteron NMR, on the other hand, is less optimal in this respect. The ^2H-NMR spectra from labeled lipids are mostly in the fast-motional limit with respect to the principal modes of molecular rotation in fluid lipid membranes. The NMR spectra are thus intrinsically less sensitive to changes in motional rates and require the combination of different relaxation experiments to describe the motion fully. This is particularly the case, for example, in the study of lipid–protein interactions, where in contrast to ESR, the NMR spectral components from the labeled lipids in environments next to and away from the intramembranous surface of integral proteins may be averaged by diffusive exchange (see, e.g., references 11–13).

A consistent description of the data from the different positions of chain labeling requires that the parameters governing the intermolecular motion of the lipid molecules, both long axis rotation and fluctuation, should be independent of the chain segment position. To do this it is found necessary to introduce the full set of six distinct orientations for any spin-labeled segment. In previous work, on the C-6 segment, it was found sufficient to include only three orientations, which minimally require one bond rotation (6). A particularly significant new result of the present work is that the flexibility gradient is found to arise not simply from an increase in the gauche probability, but also from population of the other allowed orientations (corresponding minimally to two bond rotations), on proceeding to segments closer to the terminal methyl end of the chain. This study therefore provides direct experimental evidence for the existence of these additional conformations in fluid lipid bilayers.

THEORY

Analysis of the ESR spectra of the spin-labeled phospholipid was achieved by using the density matrix formalism, outlined elsewhere (6). Here we summarize important features of this treatment and introduce the simulation parameters. The basis of our model is the stochastic Liouville equation (14, 15)

$$\frac{\partial}{\partial t}\rho(\Omega,t) = -(i/\hbar)\mathcal{H}^{\times}(\Omega) \cdot \rho(\Omega,t) - \Gamma_{\Omega} \cdot [\rho(\Omega,t) - \rho_{eq}(\Omega)], \quad (1)$$

which we solve using a finite grid point method (16, 17). Here $\rho(\Omega,t)$ represents the spin density matrix and $\mathcal{H}^{\times}(\Omega)$ is the Hamiltonian superoperator of the spin-labeled phospholipid, depending on the orientation and conformation of the molecule, specified by the Euler angles Ω. Γ_{Ω} is the time-independent Markov operator for the various motional processes and $\rho_{eq}(\Omega)$ is the equilibrium density matrix.

The model accounts for the entire dynamic range, including the slow-motional regime, where the conventional Redfield theory (18) no longer applies. The lineshapes are calculated from a spin Hamiltonian, which considers Zeeman and hyperfine interactions of nitroxide radicals, including pseudosecular contributions (19, 20). No adiabatic approximation is applied.

The Markov operator Γ_{Ω} includes both intermolecular and intramolecular motions. The intermolecular motion is the motion of the lipid molecule as a whole. It is assumed that the diffusion tensor undergoes anisotropic rotational diffusion within an orienting potential (6, 19). The intramolecular motion consists of *trans-gauche* isomerization, which is represented by a jump process (6, 21). Employing established kinetic schemes, outlined elsewhere (6), the dynamics of the system can thus be characterized by three correlation times: $\tau_{R\parallel}$ and $\tau_{R\perp}$ for rotation about the principal diffusion tensor axis and rotation of this axis, respectively, and τ_J (average residence time in one conformation) for *trans-gauche* isomerization.

The equilibrium distribution of the lipid molecules is described in terms of internal and external coordinates. The internal part accounts for different conformations and the external part for different orientations. According to the isomeric state model (21), there is only a finite number of conformational states for each nitroxide-labeled segment. Straight-forward calculation, employing rotation matrices (23), yields six allowed orientations for

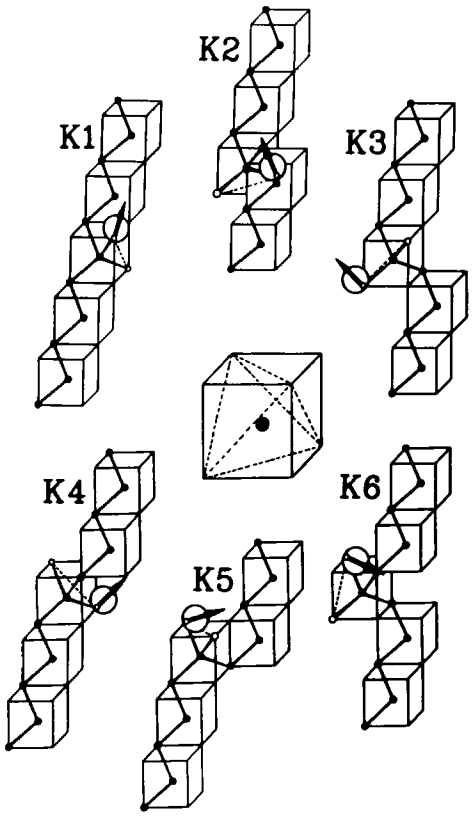

FIGURE 1 Conformational states of a phospholipid chain (C-1–C-11), nitroxide-labeled at the C-6 segment. Arrows indicate the orientation of the nitrogen hyperfine tensor (nitrogen $2p_z$ orbital). According to the isomeric state model (22), only six distinct orientations, parallel to the edges of a tetrahedron (see insert), are possible. They are each characterized by a set of Euler angles $\varphi_K, \vartheta_K, \psi_K$ ($K = 1, 2, \ldots 6$), which relate the magnetic and order tensor systems (see Fig. 2). The configurations for the two bonds immediately preceeding and immediately succeeding the labeled segment are: tttt, tg^+tg^+, g^+tg^+t, and $g^+g^+g^+t$ for the segmental orientations K1, K2, 3, K4, 5, and K6, respectively.

the magnetic tensor, defined by the NO group of the oxazolidine ring (see Fig. 1). The Euler angles $\varphi_K, \vartheta_K, \psi_K$, characterizing these orientations are listed in Table 1. The corresponding populations n_K ($K = 1, 2, \ldots 6$), giving the relative occupation probability of a particular conformational state, are normalized to unity.

In general, the *gauche* conformations at a particular segment are equally populated, corresponding to $n_2 = n_3$ and $n_4 = n_5$. From the normalization condition we obtain $n_6 = 1 - n_1 - 2(n_2 + n_4)$. Consequently, there are only three unknown populations, namely, n_1, n_2, and n_4. They may be used to set up a segmental order matrix (7) which in terms of Wigner rotation matrix averages

$$\langle D^{(2)}_{mn} \rangle = \sum_{K=1}^{6} n_K D^{(2)}_{mn}(\varphi_K \vartheta_K \psi_K) \tag{2}$$

can be written as

$$\begin{aligned}
S^K_{XX} &= (3/8)^{1/2}[\langle D^{(2)}_{02} \rangle + \langle D^{(2)}_{0\bar{2}} \rangle] - (1/2)\langle D^{(2)}_{00} \rangle \\
S^K_{YY} &= -(3/8)^{1/2}[\langle D^{(2)}_{02} \rangle + \langle D^{(2)}_{0\bar{2}} \rangle] - (1/2)\langle D^{(2)}_{00} \rangle \\
S^K_{ZZ} &= \langle D^{(2)}_{00} \rangle \\
S^K_{XY} &= i(3/8)^{1/2}[\langle D^{(2)}_{02} \rangle - \langle D^{(2)}_{0\bar{2}} \rangle] \\
S^K_{XZ} &= -(3/8)^{1/2}[-\langle D^{(2)}_{0\bar{1}} \rangle + \langle D^{(2)}_{01} \rangle] \\
S^K_{YZ} &= i(3/8)^{1/2}[\langle D^{(2)}_{01} \rangle + \langle D^{(2)}_{0\bar{1}} \rangle].
\end{aligned} \tag{3}$$

Diagonalization of $\mathbf{S}^K$ yields the segmental order parameters $S_{Z'Z'}$ and $S_{X'X'} - S_{Y'Y'}$. They express the ordering of the most-ordered segmental axis $\mathbf{Z}'$, and the anisotropy of the order, respectively. Within the limits of a completely disordered segment, all n_K are equal to 1/6, resulting in an order parameter of $S_{Z'Z'} = 0$. At the other extreme, a fully extended chain is fixed to its all-*trans* conformation, where n_1 equals unity for each segment, and the order parameter becomes $S_{Z'Z'} = 1$.

The orientational order of the lipid molecules is treated in the mean-field approximation, using an orienting

TABLE 1 Constant parameters used in the calculation of the ESR spectra of the phospholipid spin-labels 6-DMPCSL, 10-DMPCSL, and 13-CMPCSL

Hyperfine tensor	g-Tensor*	Residual line-width‡		Magnetic tensor orientations§					
		6-,10-DMPCSL	13-DMPCSL	K1	K2	K3	K4	K5	K6
mT		mT	mT						
$A_{X_KX_K} = 0.65$	$g_{X_KX_K} = 2.0088$	$(1/T^0_2)_{41} = 0.125$	$(1/T^0_2)_{41} = 0.09$	$\varphi_1 = 0°$	$\varphi_2 = -36.7°$	$\varphi_3 = 72.7°$	$\varphi_4 = -36.7°$	$\varphi_5 = 72.7°$	$\varphi_6 = -162°$
$A_{Y_KY_K} = 0.58$	$g_{Y_KY_K} = 2.0061$	$(1/T^0_2)_{52} = 0.125$	$(1/T^0_2)_{52} = 0.09$	$\vartheta_1 = 0°$	$\vartheta_2 = 60°$	$\vartheta_3 = -60°$	$\vartheta_4 = -60°$	$\vartheta_5 = 60°$	$\vartheta_6 = -90°$
$A_{Z_KZ_K} = 3.35$	$g_{Z_KZ_K} = 2.0027$	$(1/T^0_2)_{63} = 0.125$	$(1/T^0_2)_{63} = 0.09$	$\psi_1 = 0°$	$\psi_2 = -72.7°$	$\psi_3 = 36.7°$	$\psi_4 = -72.7°$	$\psi_5 = 36.7°$	$\psi_6 = -18°$

*Diagonal in $\mathbf{X}_K, \mathbf{Y}_K, \mathbf{Z}_K$.

‡$(1/T^0_2)_{ij}$ decreases with increasing temperature to a limiting value of $(1/T^0_2)_{ij} = 0.09$ mT for 6- and 10-DMPCSL and to a limiting value of $(1/T^0_2)_{ij} = 0.07$ mT for 13-DMPCSL, respectively (6).

§Euler angles relating magnetic and diffusion (order) tensor system (see Figs. 1 and 2).

potential such as is common in molecular theories of liquid crystals (24). The orientational distribution function, given elsewhere (6, 7, 25–27), is assumed to be axially symmetric and depends on only three parameters, A, δ_{min}, and δ_{max}. The coefficient A characterizes the orientation of the order tensor axis Z with respect to a local director z′ (net ordering axis), while the parameters δ_{min} and δ_{max} specify the orientation of the director axes in the sample system, defined by the glass plate normal z″ (see Fig. 2). It should be noted, that the orientational order parameter, S_{ZZ}, is related to the coefficient A by a mean value integral (28):

$$S_{ZZ} = (1/2)N_1 \int_0^{\pi} (3\cos^2\beta - 1) \exp(A\cos^2\beta) \sin\beta \, d\beta$$

$$1/N_1 = \int_0^{\pi} \exp(A\cos^2\beta) \sin\beta \, d\beta. \quad (4)$$

The microorder of the phospholipid molecules is thus specified by the orientational coefficient A plus the conformational populations n_1, n_2, and n_4, while the macroorder is specified by the values of δ_{min} and δ_{max}, characterizing the director distribution ($\delta_{min} < \delta < \delta_{max}$). In unoriented samples, the director axes z′ are randomly distributed between $\delta_{min} = 0°$ and $\delta_{max} = 180°$. In macroscopically ordered samples, however, z′ may be partially aligned, assuming a fixed tilt angle ($\delta_{min} = \delta_{max} = \delta$) relative to the glass plate normal z″ (see Fig. 2).

MATERIALS AND METHODS

Materials

Myristic acid labeled on the C-6 atom [2-(4-carboxybutyl)-2-octyl-4,4-dimethyl-3-oxazolidinyloxyl], the C-10 atom [2-(8-carboxyoctyl)-2-butyl-4,4-dimethyl-3-oxazolidinyloxyl], or the C-13 atom [2-(11-carboxyundecyl)-2-methyl-4,4-dimethyl-3-oxazolidinyloxyl] were prepared from 6-ketomyristic acid, 10-ketomyristic acid, or 13-ketomyristic acid, as described elsewhere (2, 29). Spin-labeled dimyristoylphosphatidylcholines, 1-myristoyl-2[*n*-(4,4-dimethyloxazolidine-N-oxyl)myristoyl]-*sn*-glycero-3-phosphocholines (*n*-DMPCSL), were synthesized by the catalyzed acylation of 1-myristoyl-2-lyso-*sn*-glycero-3-phosphocholine with the anhydrides of the corresponding myristic acid spin-label (30). Further details of spin-label preparation may be found in reference 29. 1,2-Dimyristoyl-*sn*-glycero-3-phosphatidylcholine (DMPC) was purchased from Fluka, Buchs, Switzerland, and the purity was controlled by thin-layer chromatography. A solvent mixture containing 75% dichloromethane and 25% methanol (vol/vol) was used to dissolve both the lipid and the spin-label. The solvents were

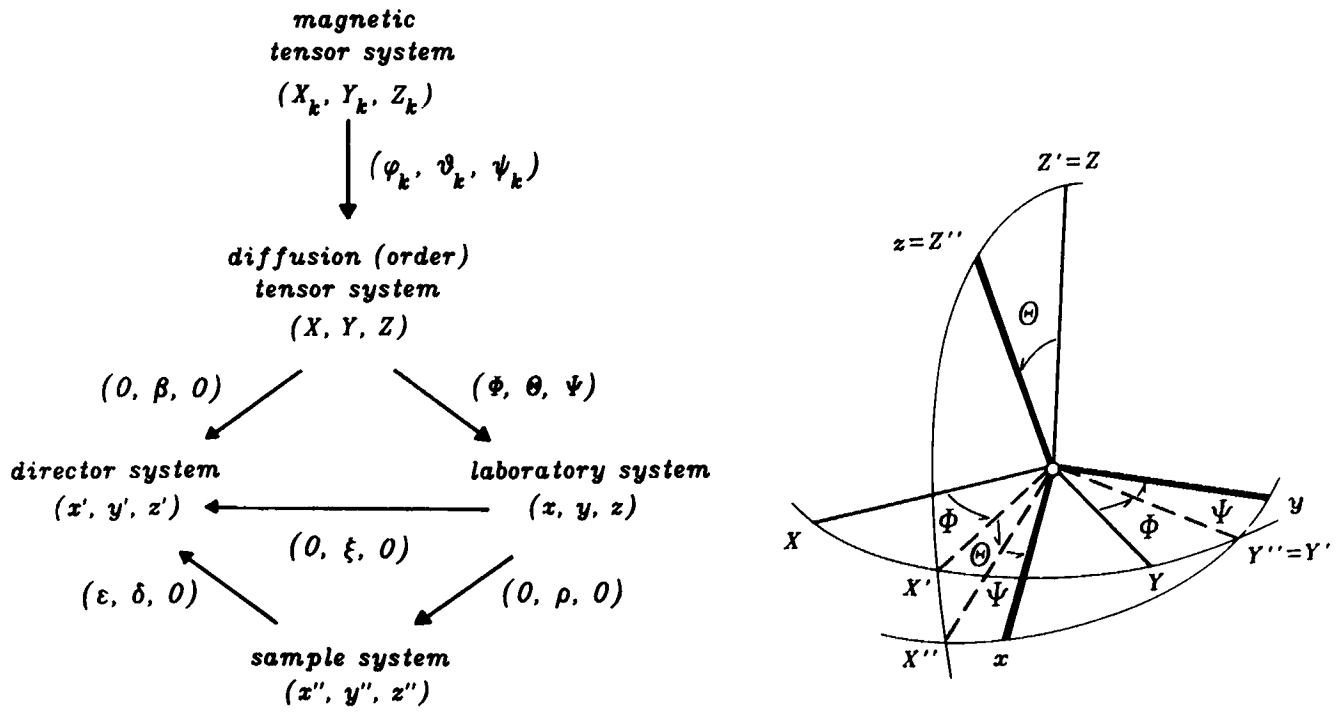

FIGURE 2 Notation for coordinate systems and Euler transformations used in the ESR line-shape model. The various coordinate systems are: Magnetic tensor system X_K, Y_K, Z_K (Z_K = direction of nitrogen $2p_z$ orbital, X_K = N—O bond direction), diffusion (order) tensor system X, Y, Z, (Z = phospholipid chain axis), laboratory system x, y, z (z = magnetic field direction), director system x′, y′, z′ (z′ = net ordering axis of phospholipid molecules), and sample system x″, y″, z″ (z″ = glass plate normal). The coordinate systems are related by Euler transformations, consisting of three successive rotations. The Euler transformation shown rotates the diffusion tensor system X, Y, Z into the laboratory system x, y, z. The definition of the Euler angles Φ, θ, Ψ corresponds to that of Van et al. (41).

distilled from KOH pellets under nitrogen atmosphere. Dichloromethane was then water saturated. All solutions were prepared immediately before use. The radical concentration was 0.2 mM, while the lipid concentration was 0.2 M.

Sample preparation

Typically, 30 μl of the above solution, corresponding to 5 nmol of spin-label and 6 μmol or 4 mg of lipid, was uniformly distributed on the bottom of an open quartz flat cell by means of a glass micropipet. The organic solvents were removed by first warming the sample cell over a waterbath (45°C, 1 min) and then placing it under vacuum (0.1 Torr, 25°C, 15 min). The cell was then placed in a water-saturated atmosphere (60°C, 1 min) and finally closed with a tightly fitting cover. The amount of water that commonly condensed onto the sample was 10 mg. The above standard procedure, developed previously (6, 25), yields macroscopically oriented multilayers of high reproducibility. The quality of the sample was checked before and after each set of ESR experiments by recording ESR spectra under the same conditions.

ESR measurements

The ESR measurements were performed on an ER 200D-SRC spectrometer (Bruker Instruments) equipped with an X-band microwave bridge (ν = 9.4 GHz), using 100-kHz field modulation. Orientation of the flat sample cell in the laboratory frame (see Fig. 2) was achieved with a home-built goniometer. ESR spectra were measured as a function of temperature and angle ρ between glass plate normal and magnetic field direction (see Fig. 2). The temperature control was found to be stable to ±0.25°C. On recording, the spectra were simultaneously digitized and transferred to an HP 1000 computer for further processing.

Spectral analysis

Fortran programs were employed to analyze the experimental spectra. The programs calculate ESR line-shapes of flexible nitroxide radicals undergoing fast, intermediate, and slow inter- and intramolecular reorientation in an anisotropic medium. On the basis of the Lanczos algorithm (31) specifically designed computer programs (LANOR 83 and NOROTJUMP 22) were found to yield accurate line-shapes with at least 10-fold reduction in computing time and computer storage requirements compared to the Rutishauser algorithm (32). Typical running time for one spectrum of the nitroxide radical on an HP 1000 computer (F series, 1.2 MByte memory) is 30 min for the L_α phase (1,350 grid points, $\tau_{R^\perp}$ = 25 ns, $\tau_{R\parallel}$ = 2.5 ns, $\tau_J < 0.1$ ns) and 480 min for the P_β and $L_{\beta'}$ phases (3,888 grid points, $\tau_{R^\perp} \simeq \tau_{R\parallel} > 100$ ns, $\tau_J = 4$ ns).

Table 1 summarizes the constant parameters used in the calculations. The magnetic parameters were obtained from a detailed analysis of fast-motional and rigid-limit spectra (6). Note that the residual line width $1/T_2^0$(isotropic) accounts for unresolved proton hyperfine interactions, omitted in the spin Hamiltonian. No Gaussian convolution was used in the spectral simulations.

The orientation of the order and diffusion tensor axes is suggested by the geometry of the spin-labeled lipid. We assume that the order tensor is axially symmetric along the phospholipid chain axis Z (see Fig. 2). This assumption, tested by spectral simulations, reflects the overall shape of the molecule, which is also expected to exhibit axially symmetric rotational diffusion about the Z axis. The magnetic tensor, defined by the NO group of the oxazolidine ring, may assume six different orientations, relative to the diffusion tensor (see Fig. 1). The Euler angles φ_K, ϑ_K, and ψ_K characterizing these orientations are also listed in Table 1.

The remaining adjustable parameters, δ_{min}, δ_{max}, A, n_1, n_2, n_4, $\tau_{R\parallel}$, $\tau_{R^\perp}$, and τ_J are determined by spectral simulations. In general, however, they need not all be evaluated. A fixed anisotropy ratio of $\tau_{R^\perp}/\tau_{R\parallel} = 10$ has previously been determined for the intermolecular motion (6), corresponding to the molecular dimensions (equivalent ellipsoid of semi-axes $a/b \sim 6$). In macroscopically unoriented samples the director axes are randomly distributed, and thus, δ_{min} and δ_{max} are known. Although this simplifies the analysis, an unambiguous fit of the remaining simulation parameters is generally not possible.

In contrast, spectral analysis of macroscopically aligned samples is unequivocal but more involved. Generally, the simulation parameters affect the line-shape in different ways. However, reliable determination of these parameters requires independent variation. Fortunately, in many cases, the director distribution is separately obtained from the angular dependence of the spectral splitting. The remaining parameters A, n_1, n_2, n_4, $\tau_{R\parallel}$, and τ_J are then evaluated by computer simulation of a set of seven angular-dependent spectra at any given temperature. An iterative fit of experimental and simulated line-shapes generally yields reliable values for all variable parameters.

In some cases, one can extract one motion, which dominates the line-shape. This is particularly true if the other motions approach either the fast motion or rigid-limit on the ESR timescale. Hence, in the L_β, and P_β, phase, where the intermolecular motions are slow, determination of the jump rates for *trans-gauche* isomerization can be achieved unambiguously. In the L_α phase, on the other hand, *trans-gauche* isomerization is too fast to be detected on the ESR timescale and thus long axis rotation and fluctuation dominate the dynamic features of the spectrum.

The particular sensitivity of the angular-dependent nitroxide ESR line-shapes to the variable parameters, characterizing molecular order and dynamics, is demonstrated elsewhere (6). It is noteworthy to realize that spectral parameters such as line intensities or line splittings do in general not relate to particular dynamic or structural features. Consequently, for systems characterized by slow motions, there is no simple strategy to elucidate the molecular properties from the spectra.

RESULTS

Macroscopically aligned samples of DMPC multibilayers were studied over a wide temperature range (2°C < T< 50°C) using three different phospholipid spin-labels. Typical ESR spectra, which vary pronouncedly with label position, temperature and orientation of glass plate normal and magnetic field, are shown in Figs. 3–5. These characterize the liquid-crystalline, L_α (Fig. 3), intermediate, P_β, (Fig. 4), and gel, $L_{\beta'}$, phases (Fig. 5) of the phospholipid membrane.

Calculated line-shapes were fitted to the experimental ones by employing the model outlined above. Note that exactly the same analysis was done on the ESR spectra as previously done on the NMR data (7, 33). However, the optimum parameters from NMR did not fit the ESR results. Numerous further calculations were then carried out, allowing for different degrees of structural and motional freedom (see, e.g., reference 6). Finally, for any given temperature only a single set of parameters was found, which faithfully reproduced all experimental spectra. The dotted lines in Figs. 3–5 represent these unique

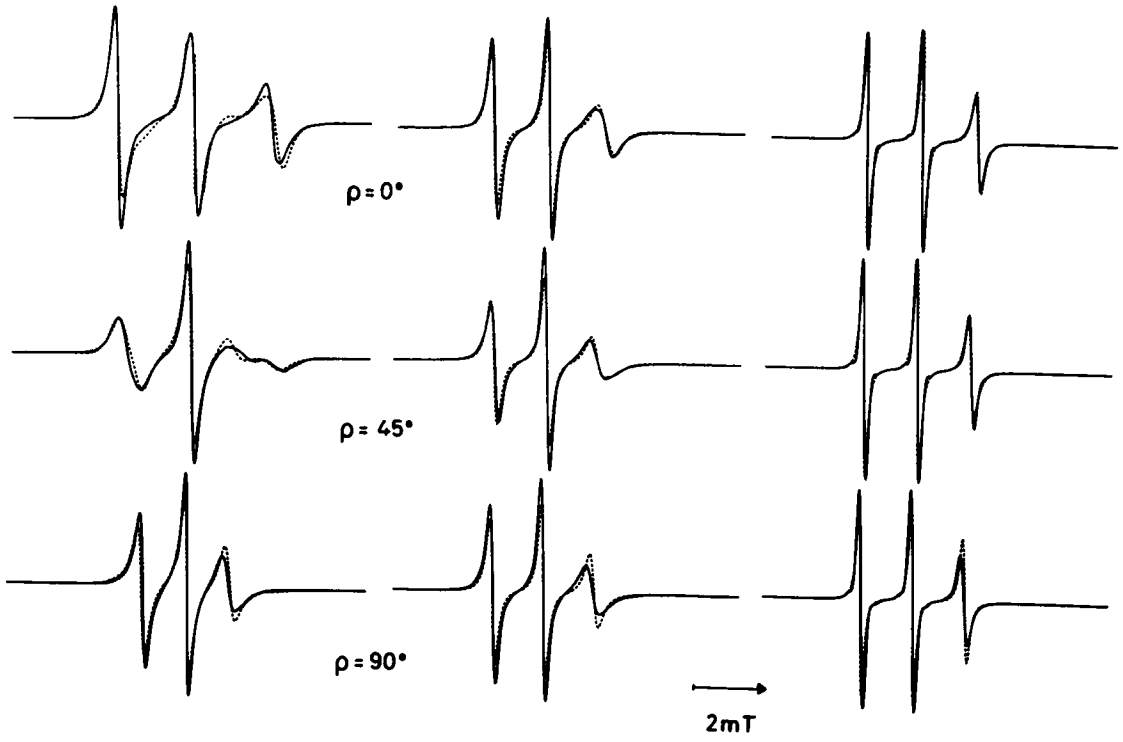

FIGURE 3 Comparison of experimental (———) and simulated (– – –) ESR spectra of 6-DMPCSL (*left column*), 10-DMPCSL (*center column*), and 13-DMPCSL (*right column*) in oriented bilayers of DMPC in the liquid crystalline phase (T = 40°C), as a function of magnetic field orientation ρ. Simulation parameters are those given in Tables 1–3 and Figs. 6–8.

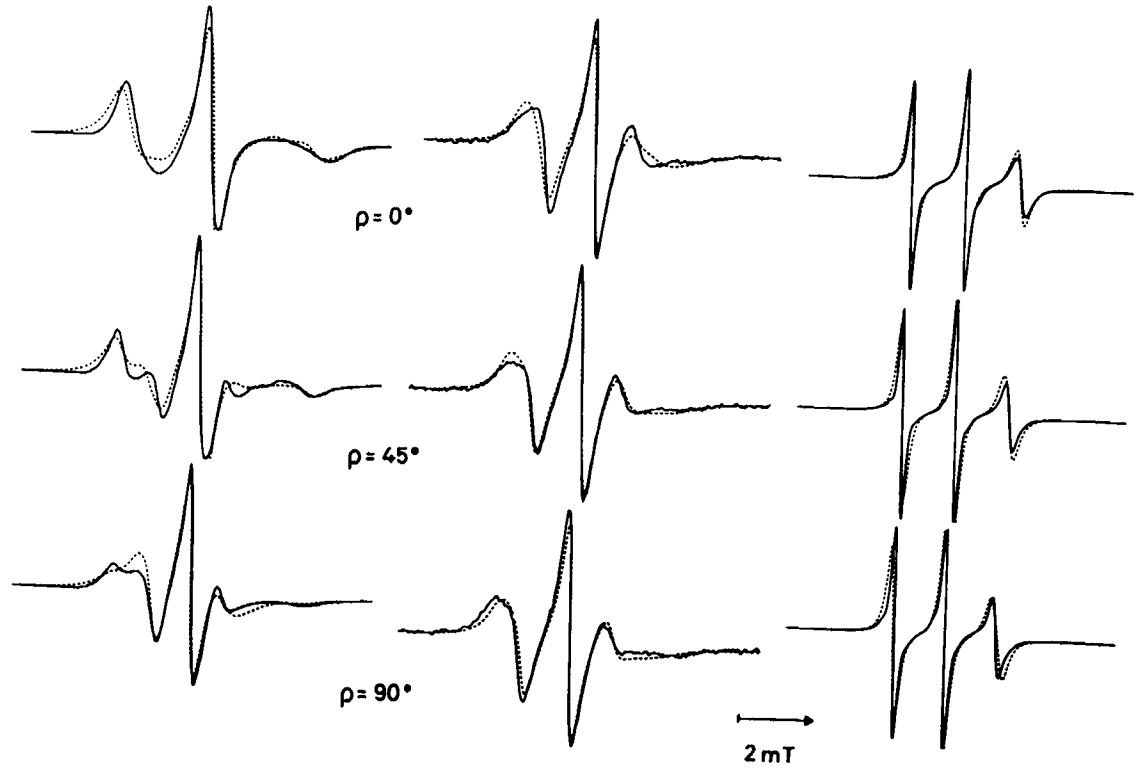

FIGURE 4 Comparison of experimental (———) and simulated (– – –) ESR spectra of 6-DMPCSL (*left column*), 10-DMPCSL (*center column*), and 13-DMPCSL (*right column*) in oriented bilayers of DMPC in the intermediate phase (T = 18°C), as a function of magnetic field orientation ρ. Simulation parameters are those given in Tables 1–3 and Figs. 6–8.

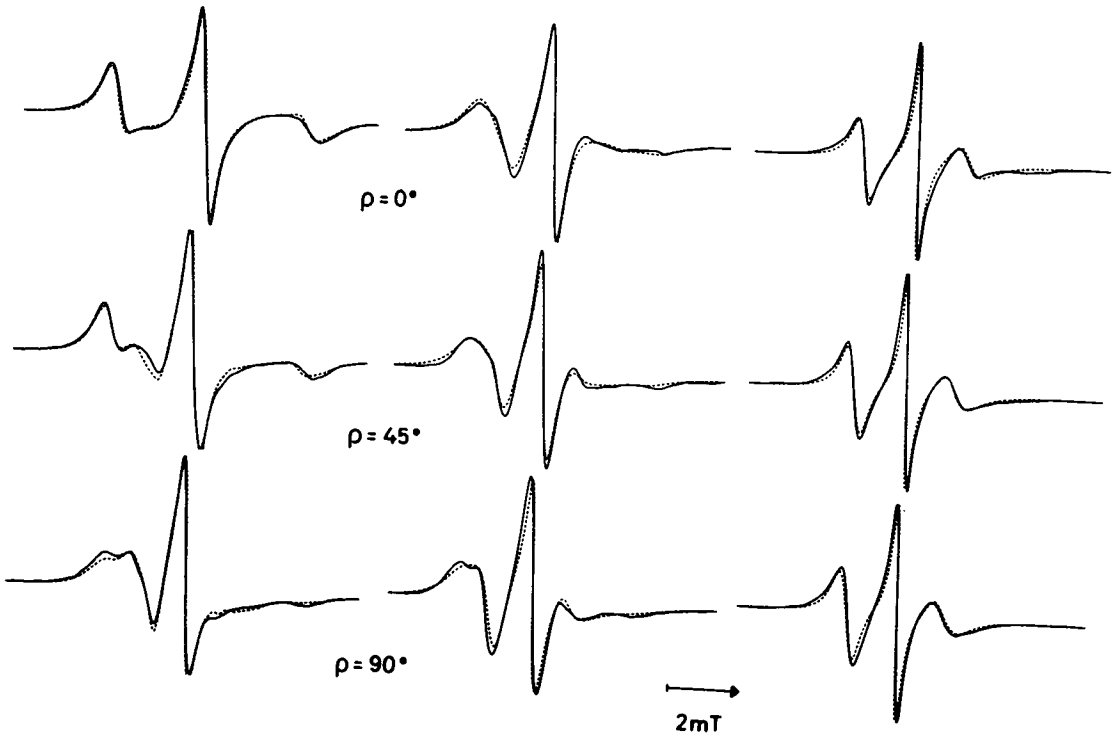

FIGURE 5 Comparison of experimental (———) and simulated (– – –) ESR spectra of 6-DMPCSL (*left column*), 10-DMPCSL (*center column*), and 13-DMPCSL (*right column*) in oriented bilayers of DMPC in the gel phase (T = 8°C), as a function of magnetic field orientation ρ. Simulation parameters are those given in Tables 1–3 and Figs. 6–8.

fits, based on the parameters of Tables 1–3 and Figs. 6–8. The agreement between experimental and calculated spectra is good. It can be improved slightly by adding spectra, to account for the <5% of unoriented material. This relatively low amount justifies the technique employed for sample preparation (25).

Note the large changes of line-shape and hyperfine anisotropy with label position for any given temperature. Whereas spectra of 6-DMPCSL show large anisotropies and appreciable slow-motional contributions in the L_α phase, spectra of 10-DMPCSL and 13-DMPCSL exhibit smaller angular dependence and sharp lines. These experimental features are unequivocal manifestations of the flexibility gradient and need to be explained in terms of molecular order and dynamics of the bilayer membrane.

The parameters characterizing the macroorder (i.e., director orientation) of the multibilayers (see Table 2) are found to be the same as in previous studies (6, 25). In the L_α phase the director orients parallel to the bilayer normal, while director axes are uniformly distributed between $\delta_{min} = 0°$ and $\delta_{max} = 25°$ in the $P_{\beta'}$ phase. In the $L_{\beta'}$ phase the director orientation changes again, showing a fixed tilt angle of $\delta_{min} = \delta_{max} = 28°$.

The temperature dependence of the microorder (orientational and segmental order parameters S_{ZZ} and $S_{Z'Z'}$) and the molecular dynamics (motional correlation times $\tau_{R^\perp}$, $\tau_{R^\parallel}$, and τ_J) is depicted in Figs. 6–8. For comparison the corresponding data from ^{2}H-NMR studies (7, 26, 33) are also plotted in these graphs. In the following we describe the results in more detail, treating molecular order and dynamics separately.

Motional correlation times

The correlation times $\tau_{R^\parallel}$, $\tau_{R^\perp}$, and τ_J refer to chain rotation about the diffusion tensor axis **Z**, reorientation of this axis, and *trans-gauche* isomerization, respectively. Logarithmic plots of these correlation times vs. $1/T$ give straight lines (see Fig. 6). From the Arrhenius plots we obtain the activation energies of the various motions, listed in Table 2.

In the L_α phase, the correlation times $\tau_{R^\parallel}$ and $\tau_{R^\perp}$ for the intermolecular lipid motion, determined by ESR, range from 1.2 to 60 ns, implying that a fast-motional line-shape theory (18) would be inadequate. The uncertainty in these correlation times is generally <10%. No dependence of the intermolecular (long axis) motion on the position of the spin-label along the phospholipid chain is detected. Correlation times $\tau_{R^\parallel}$ and $\tau_{R^\perp}$, obtained with NMR, range

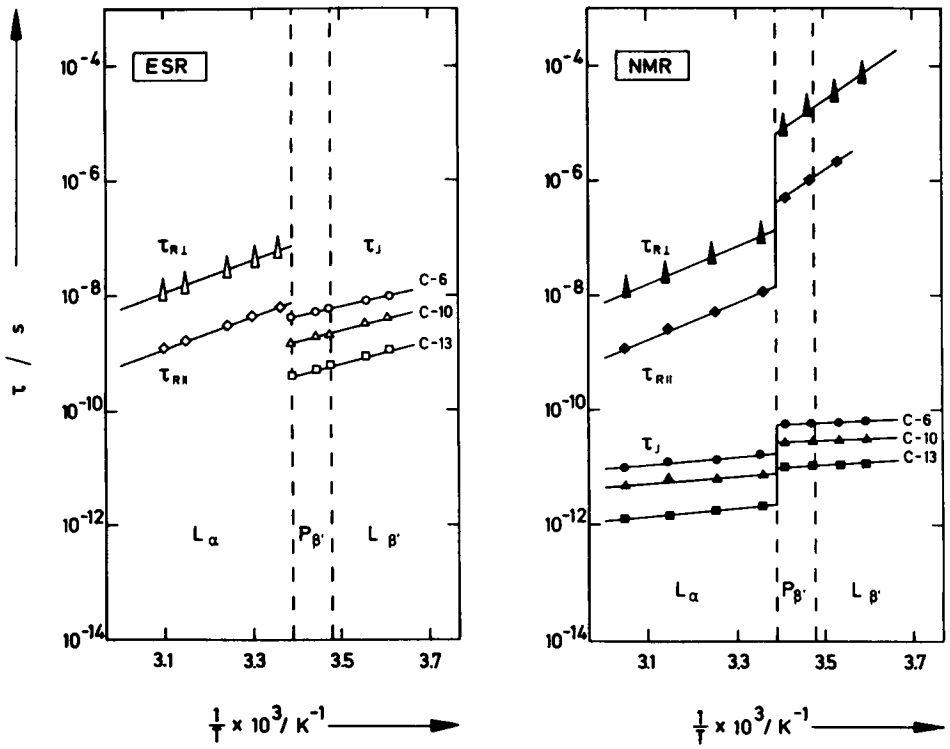

FIGURE 6 Arrhenius plots of the various correlation times, characterizing the inter- and intramolecular dynamics of DMPC membranes. The left side (*open symbols*) shows results from spin-label ESR studies, whereas the right side (*solid symbols*) represents those from ^{2}H-NMR investigations. Large triangles and diamonds refer to anisotropic overall reorientation of the phospholipid molecules, i.e., chain fluctuation and chain rotation, respectively, whereas circles, small triangles, and squares denote *trans-gauche* isomerization at the C-6, C-10, and C-13 segments, respectively. Dashed lines indicate different phase transitions (L_α = liquid crystalline phase, $P_{\beta'}$ = intermediate phase, and $L_{\beta'}$ = gel phase).

from 1.1 to 100 ns and do not depend on the label position. This result is in accordance with the ESR measurements.

Trans-gauche isomerization of the nitroxide-labeled lipid in the L_α phase can only be characterized by a limiting correlation time $\tau_J \leqq 0.2$ ns, since it exhibits no other effect than fast exchange of the respective conformations on the ESR time scale. In contrast, NMR is able to evaluate the intramolecular dynamics by T_{1Z} relaxation with correlation times τ_J ranging from 1 to 16 ps. Furthermore, a dependence of the *trans-gauche* isomerization rate on the label position is detected by NMR, exhibiting considerably faster motion towards the end of the phospholipid chain (33).

At the main transition, the correlation times for all three motions decrease significantly. On the ESR time scale, τ_{R^I} and $\tau_{R^\perp}$ are now in the rigid-limit and cannot be determined anymore. From ^{2}H-NMR studies of the $P_{\beta'}$ phase, the correlation times for chain rotation and chain fluctuation are found to range from 500 ns $\leqq \tau_{R^I} \leqq$ 1,020 ns and from 8 μs $\leqq \tau_{R^\perp} \leqq$ 15.5 μs, practically independent of ^{2}H label position (7, 33). This is consistent with the ESR result.

The only dynamic process, affecting the ESR line-shape in the $P_{\beta'}$ phase, is *trans-gauche* isomerization with correlation times τ_J of 4.3, 2.0, and 0.5 ns for the C-6, C-10, and C-13 segment, respectively, at 18°C. Indeed these correlation times can now be determined precisely from simulations of the ESR line-shape. The maximum error for the conformational lifetimes is <10%. In comparison, correlation times for *trans-gauche* isomerization from ^{2}H-NMR experiments are found to be τ_J = 36 ps, τ_J = 22 ps, and τ_J = 14 ps at 18°C, respectively (33). It appears that intramolecular motion of the nitroxide-labeled lipid is slowed down considerably when compared to the pure system.

For *trans-gauche* isomerization, no significant discontinuity in motional rates is found at the pretransition with either method (ESR or NMR) when the experiment is performed without prior incubation at 0°C for several days (cf. reference 34). The correlation times τ_J of the nitroxide-labeled lipid amount to 8, 4, and 1 ns for 6-DMPCSL, 10-DMPCSL, and 13-DMPCSL at 8°C, respectively. They are at least two orders of magnitude slower than those deduced from ^{2}H-NMR studies (33).

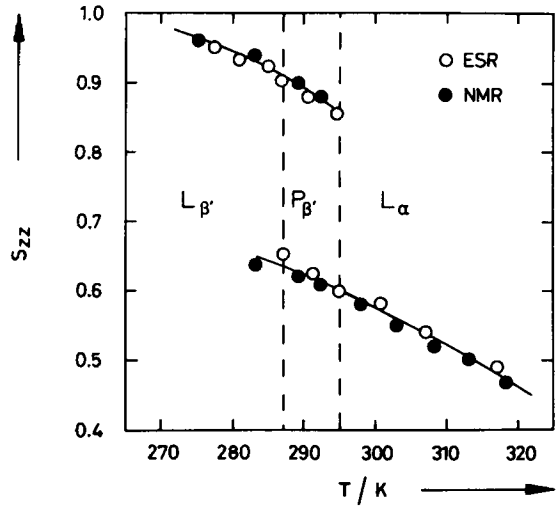

FIGURE 7 Temperature dependence of the orientational order in DMPC membranes, expressed in terms of chain order parameters S_{ZZ}, characterizing the average orientation of the phospholipid molecules with respect to the director. Open symbols refer to measurements, employing various ESR spin-labels, while solid symbols denote measurements using ^{2}H-NMR spin-labels. Dashed lines indicate different phase transitions (L_α = liquid crystalline phase, $P_{\beta'}$ = intermediate phase, $L_{\beta'}$ = gel phase).

Order parameters

The orientational order parameter S_{ZZ} of the lipid molecules, determined from the ESR studies, increases with decreasing temperature from $S_{ZZ} = 0.47$ to $S_{ZZ} = 0.59$ in the L_α phase. The values are independent of the spin-label position along the phospholipid chain.

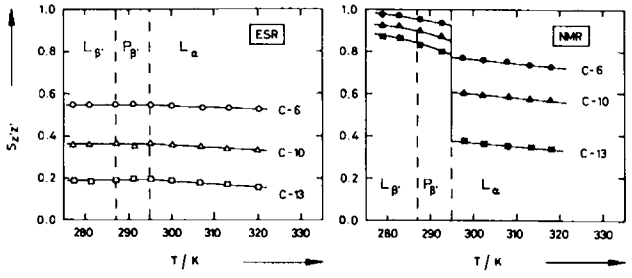

FIGURE 8 Temperature dependence of the conformational order in DMPC membranes, expressed in terms of segmental order parameters $S_{Z'Z'}$ at various chain segments. $S_{Z'Z'}$ characterizes the ordering of the most-ordered segmental axis. The left side (*open symbols*) shows results from spin-label ESR studies, whereas the right side (*solid symbols*) represents those from ^{2}H-NMR investigations. Circles refer to the C-6 segment, whereas triangles and squares denote the segmental order of the C-10 and C-13 segments, respectively. Dashed lines indicate different phase transitions (L_α = liquid crystalline phase, $P_{\beta'}$ = intermediate phase, $L_{\beta'}$ = gel phase).

From analysis of biradical ESR and ^{2}H-NMR spectra, it was found that the system is heterogeneous in the $P_{\beta'}$ phase as two different components are observed (7, 25, 26). Appropriate simulation of these components in the ^{2}H-NMR spectra is only possible with different order parameters of $S_{ZZ} \simeq 0.6$ and $S_{ZZ} \simeq 0.9$, corresponding to those determined in the L_α and $L_{\beta'}$ phases, respectively. Consideration of this heterogeneity provides good spectral fits for the ESR spectra, discussed in this paper. In the $L_{\beta'}$ phase, we observe only a minor temperature dependence of the chain order parameter S_{ZZ}, approaching a value close to unity at $T \simeq 0$°C. Generally, there is good agreement between orientational order parameters from spin-label ESR and ^{2}H-NMR studies (see Fig. 7).

This, however, does not apply to the segmental order parameters $S_{Z'Z'}$ at the various chain positions, although in both cases the gauche probability increases towards the end of the chain, resulting in a significant decrease of $S_{Z'Z'}$. In the L_α phase ($T = 40$°C), the segmental order parameters from spin-label ESR are $S_{Z'Z'} = 0.54$, $S_{Z'Z'} = 0.34$, and $S_{Z'Z'} = 0.17$ at the C-6, C-10, and C-13 segment, respectively. In contrast, ^{2}H-NMR studies yield substantially higher values at the corresponding positions (7, 33), namely $S_{Z'Z'} = 0.74$, $S_{Z'Z'} = 0.56$, and $S_{Z'Z'} = 0.35$ ($T = 40$°C). In addition, the segmental order parameters from ^{2}H-NMR exhibit a more pronounced temperature dependence than those from ESR (see Fig. 8).

Table 3 summarizes the parameters, characterizing the order gradient in the L_α phase, i.e., the conformational populations $n_1, n_2 \cdots n_6$, the segmental order parameter $S_{Z'Z'}$, and the orientational order parameter S_{ZZ}. The maximum error for both types of order parameters is generally <6%. The results are compared with a corresponding analysis of the ^{2}H-NMR of DMPC bilayers labeled at the same methylene segments (7, 33). Inspection of Table 3 reveals that the parameters governing orientational order are in good agreement, whereas the segmental order parameters differ significantly.

Interestingly, $S_{Z'Z'}$, obtained from spin-label ESR, remains fairly constant over the whole temperature range investigated (2°C $\leq T \leq$ 50°C). In contrast, ^{2}H-NMR indicates a discontinuity in S_{ZZ} at the main transition to considerably higher values of $S_{Z'Z'} = 0.95$, $S_{Z'Z'} = 0.87$, and $S_{Z'Z'} = 0.80$ for positions 6, 10, and 13, respectively. No discontinuity is detected at the pretransition, with the segmental order parameter $S_{Z'Z'}$ approaching values between 0.9 and 0.98, depending on the position of the ^{2}H label along the chain (7, 33).

DISCUSSION

This work combines the information obtained from three different positions of labeling to parameterize a motional

TABLE 2 Structural and dynamic parameters for the various phases of DMPC bilayers, determined by spin-label ESR

Phase	Director distribution*		Rotational activation energies‡				
	δ_{min}	δ_{max}	E_J (C-6)	E_J(C-10)	E_J(C-13)	$E_{R^\perp}$	$E_{R^\parallel}$
					kcal/mol		
L_α	0°	0°	—	—	—	11.8 ± 0.5	11.8 ± 0.5
$P_{\beta'}$	0°	25°	5.3 ± 0.7	4.5 ± 0.7	3.7 ± 0.7	—	—
$L_{\beta'}$	28°	28°	5.3 ± 0.7	4.5 ± 0.7	3.7 ± 0.7	—	—

*The uncertainty in fixed tilt angles ($\delta_{min} - \delta_{max}$) is ≤5°.
‡E_J is the activation energy for *trans-gauche* isomerization of the particular labeled segment; $E_{R^\perp}$ and $E_{R^\parallel}$ refer to fluctuation and rotation of the phospholipid molecule as a whole.

model which involves both overall lipid reorientation and segmental chain isomerism. The aim was both to test previous results obtained with a single chain labeling position (6) and to provide information on the chain flexibility gradient. The fact that a consistent description of the overall lipid motion can be obtained for all positions of labeling further supports the motional model. It also further demonstrates the ability to discriminate between the motional modes by simulation of an extensive angular dependence and temperature dependence of the spectra from oriented samples. The temperature dependence yields activation energies (Table 2) which clearly distinguish the intramolecular from the intermolecular motion. The segmental motion has activation energies which are comparable to the barrier height for *trans-gauche* isomerism (1), whereas the activation energies for the overall lipid motion are two to three times greater. The small increase in E_J from the C-13 to the C-6 position most probably reflects the prevalence of coupled rotations, as opposed to isolated bond rotations, for the chain segments closer to the polar group region. The activation energies for chain rotation ($E_{R^\parallel}$) and for chain fluctuation ($E_{R^\perp}$) given in Table 2 are necessarily equal, because of the constant anisotropy ratio $\tau_{R^\perp}/\tau_{R^\parallel}$ determined previously (6). The discrimination between the inter- and intramolecular motions is also seen in the temperature dependence of the order parameters (Figs. 7 and 8), which is much greater for the intermolecular case. The temperature dependence of the segmental order parameter is essentially determined by the energy difference between the trans and gauche conformations of ~0.5 kcal/mol (1), whereas that of the orientational order parameter is determined by the orientational potential (see Eq. 3).

To obtain a consistent interpretation of the data from the label positions closer to the terminal methyl end of the chain, it is necessary to take into account all the distinct orientations which the nitrogen hyperfine tensor of the labeled segment may take up. For sp^3 bond symmetry, these correspond to the edges of a tetrahedron, as indicated in Fig. 1. There are 12 distinct orientations in all, allowing for the two opposing directions along each axis. But only six need to be considered, since magnetic resonance spectra are not able to distinguish the two sets of opposing orientations. The first three conformational orientations in Fig. 1 are generated essentially by a rotation about only the C—C bond immediately adjacent to the chain segment. K1 has a *trans* conformation, and K2, K3 have *gauche*± conformations, about this bond. In

TABLE 3 The flexibility gradient in the liquid crystalline phase (T = 40°C) of DMPC membranes, determined by spin-label ESR and deuteron NMR

Chain segment	Spin-label ESR*								Deuteron NMR‡					
	Populations of conformational states§						Order parameters‖		Populations of conformational states¶				Order parameters‖	
	n_1	n_2	n_3	n_4	n_5	n_6	$S_{Z'Z'}$	S_{ZZ}	$n_{1'}$	$n_{2'}$	$n_{3'}$	$n_{4'}$	$S_{Z'Z'}$	S_{ZZ}
C-6	0.50	0.25	0.25	0.00	0.00	0.00	0.54	0.50	0.80	0.10	0.10	0.00	0.74	0.50
C-10	0.18	0.30	0.30	0.11	0.11	0.00	0.34	0.50	0.66	0.14	0.14	0.06	0.56	0.50
C-13	0.18	0.24	0.24	0.14	0.14	0.06	0.17	0.50	0.51	0.18	0.18	0.13	0.35	0.50

*Data from this study.
‡Data from Meier et al. (7) and Mayer et al. (33).
§The numbers denote the six distinct orientations of the nitrogen hyperfine tensor, according to the isomeric state model (22, 23).
‖The segmental order parameter $S_{Z'Z'}$ expresses the ordering of the most ordered segmental axis Z' with respect to the order tensor axis Z; the orientational order parameter S_{ZZ} characterizes the average orientation of Z with respect to the director z' (see Fig. 2).
¶The numbers denote the four distinct orientations of deuteron quadrupole coupling tensor, according to the isomeric state model (7, 22).

the notation of Meraldi and Schlitter (35), the K1, K2, and K3 configurations correspond to the (t, 0°), and ($g^{\pm}$, 60°) conformers, where the angle corresponds to the orientation of the chain segment relative to the initial trans segments. The second three conformational orientations in Fig. 1 are generated essentially by rotations about the two C—C bonds immediately preceding the labeled chain segment. K4 and K5 correspond to the *gauche*$^{\pm}$-*trans*, i.e. (t, 60°), combinations, and K6 corresponds to the *gauche*$^{+}$-*gauche*$^{+}$, i.e. (g^{+}, 90°), combination. Additional gauche rotations have been included in the configurations K2 to K6 simply to maintain approximate linearity of the chain axis. For configurations K2 to K5 these correspond to classical kink sequences. (The configurations for the two bonds immediately preceeding and immediately succeeding the labeled segment are: tttt, $tg^{\pm}tg^{\mp}$, $g^{\pm}tg^{\mp}t$ and $g^{+}g^{+}g^{+}t$ for the configurations K1, K2, 3, K4, 5, and K6, respectively.) The six conjugate, indistinguishable orientations would correspond to the set (t, 180°), ($g^{\pm}$, 120°), (t, 120°), and (g^{-}, 90°).

The results of the simulations show that only the first three configurations (K1–K3), which require only a single rotation immediately preceeding the segment, are appreciably populated at the C-6 segment. At the C-10 segment, the two conformations K4 and K5, which require rotations about the two bonds immediately preceding the segment, are additionally populated. Only at the C-13 segment is the K6 conformation, which not only requires two rotations but also requires both to be *gauche*, appreciably populated. Thus the flexibility gradient involves an increasing probability of *gauche* conformations on proceeding down the chain from the polar interface. This is demonstrated by the fact that the probability for a *gauche* conformation occurring two bonds ahead becomes non-zero on going from the C-6 to the C-10 segment. An additional contribution to the flexibility gradient is the non-vanishing probability for adjacent gauche conformations, which occurs only very close to the terminal methyl end of the chain, i.e., at the C-13 segment, here.

Apparently, there is an order or flexibility gradient along the chains for both the nitroxide- and deuterium-labeled membranes. Table 3 summarizes the results for the C-6, C-10, and C-13 segments, respectively. Note that the populations n_1–n_6 and $n_{1'}$–$n_{4'}$ of all conformational states, accessible at a particular segment, are presented. Interpretation of these chain segment conformations in terms of statistical mechanical models is a challenging theoretical problem (35–38).

Comparison of the ESR and the NMR data reveals that the spin-label spectra faithfully reflect the overall motion of the lipid molecules. This is true both for the intermolecular dynamics (Fig. 6) and for the orientational order (Fig. 7). The segmental motion is very different, however, for the spin-labeled and deuterium-labeled chains (Figs. 6 and 8). Because the nitroxide and CD-bond axes are differently oriented, they transform differently with the various chain conformations and reflect different elements of the conformational order (7, 39). For this reason, the segmental ordering tensor has been evaluated in both systems. This then affords a relatively direct comparison between the two sets of data. As found previously for the C-6 segment, the segmental order is considerably lower for the ESR label than for the NMR label at all three chain positions. The origin of this difference is almost certainly a local distortion of the chain conformation at the position of the nitroxide group, for the same reasons as those advanced in the discussion of the C-6 data (6, 40). Thus the ESR spectra directly reflect the motions of the whole molecule, but only indirectly those of the chain conformations.

Use of oriented samples allows one to specify the macroorder of the lipid molecules (i.e., director axis distribution), relative to the bilayer normal. Identical values are obtained at all label positions in the chain, thus further substantiating the model used for the spectral simulation. A fixed tilt is observed in the gel phase, a distribution of tilt angles is found in the intermediate phase, and no net tilt is detected in the fluid phase. As discussed previously (6), these results are quantitatively in agreement with the values obtained from x-ray diffraction in the gel and intermediate phases (4, 5). Spin-label ESR has the additional advantage over x-ray diffraction, that data may also be obtained from the fluid phase.

CONCLUSIONS

In summary, a consistent description has been obtained of the ESR spectra from lipids labeled at different positions in the hydrocarbon chain, using a model which includes whole-body motions and chain isomerism. To interpret results from label positions closer to the terminal methyl group of the chains, it is necessary to introduce the complete set of six independent orientations of the hyperfine tensor, and not simply the three isolated *trans* and *gauche* conformers. All these different conformations are allowed on theoretical grounds, and the magnetic resonance experiments reported here provide direct evidence for their presence in fluid lipid bilayers. The overall lipid motions lie in the slow to intermediate regime of conventional ESR spectroscopy and thus can be characterized relatively precisely by spectral simulations. These results are in good agreement with those obtained from ^{2}H-NMR spectroscopy, for which these motions are in the fast regime. The segmental motions are sensitive to the local distorting effect of the nitroxide ring, but nonetheless provide an empirical means of characterizing the

chain flexibility gradient. As in undistorted membrane systems, there is a strong decrease of the segmental order on going down the chain from the polar interface. Close to the terminal methyl end all conformational states of the nitroxide-labeled segment are almost equally populated, giving rise to sharp angular-independent ESR lines. These results are of direct relevance to the interpretation of spin-label ESR spectra from more complex membrane systems such as lipid–protein recombinants, and combined with the NMR results provide fundamental data for the construction of statistical mechanical models of the lipid bilayer.

We thank Frau B. Angerstein for her chemical expertise in the preparation of the spin-labels and Dr. E. Ohmes for his assistance in the computations.

Financial support by Deutsche Forschungsgemeinschaft and Fonds der Chemischen Industrie is gratefully acknowledged.

Received for publication 25 April 1988 and in final form 23 September 1988.

REFERENCES

1. Cevc, G., and D. Marsh. 1987. Phospholipid Bilayers. Physical Principles and Models. Wiley-Interscience, New York. 442 pp.
2. Hubbell, W. L., and H. M. McConnell. 1971. Molecular motion in spin labeled phospholipids and membranes. *J. Am. Chem. Soc.* 93:314–326.
3. Seelig, A., and J. Seelig. 1974. The dynamic structure of fatty acyl chains in a phospholipid bilayer measured by deuterium magnetic resonance. *Biochemistry.* 13:4839–4845.
4. Janiak, M. J., D. M. Small, and G. G. Shipley. 1976. Nature of the thermal pretransition of synthetic phospholipids: dimyristoyl- and dipalmitoyllecithin. *Biochemistry.* 15:4575–4580.
5. Inoko, Y., and T. Mitsui. 1978. Structural parameters of dipalmitoylphosphatidylcholine lamellar phases and bilayer phase transitions. *J. Phys. Soc. Jpn.* 44:1918–1924.
6. Lange, A., D. Marsh, K.-H. Wassmer, P. Meier, and G. Kothe. 1985. Electron spin resonance study of phospholipid membranes employing a comprehensive line-shape model. *Biochemistry.* 24:4383–4392.
7. Meier, P., E. Ohmes, and G. Kothe. 1986. Multipulse dynamic nuclear magnetic resonance of phospholipid membranes. *J. Chem. Phys.* 85:3598–3614.
8. Schindler, H., and J. Seelig. 1975. Deuterium order parameters in relation to thermodynamic properties of a phospholipid bilayer. A statistical mechanical interpretation. *Biochemistry.* 14:2283–2287.
9. Tanaka, H., and J. H. Freed. 1984. Electron spin resonance studies on ordering and rotational diffusion in oriented phosphatidylcholine multilayers: evidence for a new chain-ordering transition. *J. Phys. Chem.* 88:6633–6644.
10. Kar, L., Ney-Igner, E., and J. H. Freed. 1985. Electron spin resonance and electron-spin-echo study of oriented multibilayers of L_α-dipalmitoylphosphatidylcholine water systems. *Biophys. J.* 48:569–595.
11. Seelig, J., A. Seelig, and L. Tamm. 1982. Nuclear magnetic resonance and lipid-protein interactions. *In* Lipid–Protein Interactions. Vol. 2. P.C. Jost and O.H. Griffith, editors. Wiley-Interscience, New York. 127–148.
12. Bloom, M., and I. C. P. Smith. 1985. Manifestations of lipid-protein interactions in deuterium NMR. *In* Progress in Protein–Lipid Interactions. Vol. 1. A. Watts and J. J. H. H. M. DePont, editors. Elsevier, Amsterdam. 61–88.
13. Marsh, D., and A. Watts. 1989. Association of lipids with membrane proteins. *In* Advances in Membrane Fluidity. Vol. 2. R. C. Aloia, C. C. Curtain, and L. M. Gordon, editors. Alan R. Liss, New York. In press.
14. Kubo, R. 1969. A stochastic theory of lineshape. *In* Stochastic Processes in Chemical Physics: Advances in Chemical Physics. K. E. Shuler, editor. John Wiley & Sons, Inc., New York. 101–127.
15. Freed, J. H., G. V. Bruno, and C. F. Polnaszek. 1971. Electron spin resonance lineshapes and saturation in the slow motional region. *J. Phys. Chem.* 75:3385–3399.
16. Norris, J. R., and S. I. Weissman. 1969. Studies of rotational diffusion through electron-electron dipolar interactions. *J. Phys. Chem.* 73:3119–3124.
17. Kothe, G. 1977. Electron spin resonance of symmetrical three spin systems in nematic liquid crystals. II. Slow-motional spectra. *Mol. Phys.* 33:147–158.
18. Redfield, A. G. 1965. The theory of relaxation processes. *Adv. Magn. Reson.* 1:1–32.
19. Freed, J. H. 1976. Theory of slow tumbling ESR spectra for nitroxides. *In* Spin Labeling. Theory and Applications. Vol. 1. L. J. Berliner, editor. Academic Press, Inc., New York. 53–132.
20. Wassmer, K.-H., E. Ohmes, M. Portugall, H. Ringsdorf, and G. Kothe. 1985. Molecular order and dynamics of liquid-crystal side-chain polymers: an electron spin resonance study employing rigid nitroxide spin probes. *J. Am. Chem. Soc.* 107:1511–1519.
21. Luz, Z. 1985. Dynamics of molecular processes by NMR in liquid crystalline solvents. *In* Nuclear Magnetic Resonance of Liquid Crystals. J. W. Emsley, editor. D. Reidel Publishing Company, Dordrecht. 315–342.
22. Flory, P. J. 1969. Statistical Mechanics of Chain Molecules. Wiley-Interscience, New York. 338 pp.
23. Moser, M. 1985. Elektronenspinresonanz-Untersuchungen zum Flexibilitätsgradienten in Phospholipidmembranen. Diploma thesis, University of Stuttgart. 31 pp.
24. Cotter, M. A. 1977. Hard spherocylinders in an anisotropic mean field: a simple model for a nematic liquid crystal. *J. Chem. Phys.* 66:1098–1106.
25. Meier, P., A. Blume, E. Ohmes, F. A. Neugebauer, and G. Kothe. 1982. Structure and dynamics of phospholipid membranes: an electron spin resonance study employing biradical probes. *Biochemistry.* 21:526–534.
26. Meier, P., E. Ohmes, G. Kothe, A. Blume, J. Weidner, and H.-J. Eibl. 1983. Molecular order and dynamics of phospholipid membranes. A deuteron magnetic resonance study employing a comprehensive line-shape model. *J. Phys. Chem.* 87:4904–4912.
27. Müller, K., P. Meier, and G. Kothe. 1985. Multipulse dynamic NMR of liquid crystal polymers. *Prog. Nucl. Magn. Reson. Spectrosc.* 17:211–239.
28. Saupe, A. 1964. Kernresonanzen in kristallinen Flüssigkeiten und kristallinflüssigen Lösungen. *Z. Naturforsch.* 19A: 161–171.

29. Marsh, D., and A. Watts. 1982. Spin labeling and lipid-protein interactions in membranes. *In* Lipid-Protein Interactions. Vol. 2. P.C. Jost and O. H. Griffith, editors. Wiley-Interscience, New York. 53–126.

30. Mason, J. T., A. V. Broccoli, and C. Huang. 1981. A method for the synthesis of isomerically pure saturated mixed chain phosphatidylcholines. *Anal. Biochem.* 113:96–101.

31. Moro, G., and J. H. Freed. 1981. Calculation of the ESR spectra and related Fokker-Planck forms by the use of the Lanczos algorithm. *J. Chem. Phys.* 74:3757–3773.

32. Gordon, R. G., and J. Messenger. 1972. Magnetic resonance line shapes in slowly tumbling molecules. *In* Electron Spin Relaxation in Liquids. L. T. Muus and P. W. Atkins, editors. Plenum Publishing Corp., New York. 341–381.

33. Mayer, C., K. Müller, K. Weisz, and G. Kothe. 1988. Deuteron NMR relaxation studies of phospholipid membranes. *Liquid Crystals.* 2:797–806.

34. Finegold, L., and M. A. Singer. 1986. The metastability of saturated phosphatidylcholines depends on the acyl chain length. *Biochim. Biophys. Acta.* 855:417–420.

35. Meraldi, J. P., and J. Schlitter. 1981. A statistical mechanical treatment of fatty acyl chain order in phospholipid bilayers and correlation with experimental data. B. Dipalmitoyl-3-*sn*-phosphatidyl-choline. *Biochim. Biophys. Acta.* 645:183–210.

36. Marcelja, S. 1974. Chain ordering in liquid crystals. II. Structure of bilayer membranes. *Biochim. Biophys. Acta.* 367:165–176.

37. Jähnig, F. 1979. Molecular theory of lipid membrane order. *J. Chem. Phys.* 70:3279–3290.

38. Dill, K. A., and P. J. Flory. 1980. Interphases of chain molecules: monolayers and lipid bilayer membranes. *Proc. Natl. Acad. Sci. USA.* 77:3115–3119.

39. Marsh, D. 1985. ESR probes for structure and dynamics of membranes. *In* Spectroscopy and the Dynamics of Biological Systems. P. M. Bayley and R. E. Dale, editors. Academic Press, London. 209–238.

40. Taylor, M. G., and I. C. P. Smith. 1983. The conformations of nitroxide-labeled fatty acid probes of membrane structure as studied by ^{2}H-NMR. *Biochim. Biophys. Acta.* 733:256–263.

41. Van. S. P., G. B. Birrell, and O. H. Griffith. 1974. Rapid anisotropic motion of spin labels. Models for motion averaging of the ESR parameters. *J. Magn. Reson.* 15:444–459.